

August 2004

# Detection of sleptons at a linear collider in models with small slepton-neutralino mass differences<sup>\*</sup>

Hans-Ulrich Martyn<sup>†</sup>

*I. Physikalisches Institut, RWTH Aachen, Germany*

A feasibility study is presented to precisely measure the masses of charged sleptons and the lightest neutralino in  $e^+e^- \rightarrow \tilde{\mu}_R\tilde{\mu}_R$  and  $e^+e^- \rightarrow \tilde{\tau}_1\tilde{\tau}_1$  production. Different mSUGRA scenarios with small slepton-neutralino mass differences of a few GeV are investigated. The analysis is based on a detailed simulation of the final state lepton energy spectra including background reactions and assuming realistic experimental conditions at the TESLA  $e^+e^-$  Linear Collider. Effects on the mass resolutions due to beams colliding head-on or under a crossing angle are discussed.

## 1 Introduction

In the minimal supersymmetric standard model the lightest superparticle (LSP), which is stable in  $R$ -parity conserving scenarios, is a natural candidate for cold dark matter. Measurements of the WMAP experiment [1] have determined the amount of cold dark matter in the universe to be  $\Omega_{CDM}h^2 = 0.113 \pm 0.009$ . As a consequence of this result, considerable constraints on the parameters of supersymmetric theories can be set [2]. For example, in minimal supergravity (mSUGRA), where usually the LSP is the neutralino  $\tilde{\chi}_1^0$ , the favoured particle spectra are typically characterised by small mass differences between the lightest slepton (usually the stau) and neutralino (coannihilation region) or between the light chargino and neutralino (focus point region). Collider experiments will be essential to test the supersymmetry dark matter hypothesis. But only a future  $e^+e^-$  Linear Collider will be able to provide precise enough mass measurements of the light SUSY particles in order to compute the relic density of the LSP to an accuracy comparable with WMAP and other proposed experiments.

Experimentally challenging is the coannihilation region where the slepton-neutralino mass difference  $\Delta m$  may be as small as a few GeV. In this note we investigate the capabilities of a

---

<sup>\*</sup>Contribution to the ECFA Study on Physics and Detectors for a Linear Collider and the International Conference on Linear Colliders, LCWS 04, Paris, April 2004

<sup>†</sup>email: martyn@mail.desy.de

TeV  $e^+e^-$  Linear Collider like TESLA [3] to detect and measure  $\tilde{\mu}_R\tilde{\mu}_R$  and  $\tilde{\tau}_1\tilde{\tau}_1$  pair production in models with small  $\Delta m$  in order to determine precisely the masses of the light sleptons as well as of the neutralino  $\tilde{\chi}_1^0$  from the energy spectra of the final states. The case studies are based on spectra from a SPS 1a inspired model [4], where the neutralino mass has been increased to accommodate a small mass difference  $\Delta m$  and from the benchmark model D' proposed in [5].

The most severe background comes from four fermion production via two-photon ( $\gamma\gamma$ ) processes,  $e^+e^- \rightarrow e^+e^-f\bar{f}$ , and it is important to have an efficient veto of the spectator electrons/positrons down to very small scattering angles. The present study also addresses the consequences for background suppression in head-on collisions, as envisaged in the TESLA design, versus the option of having a crossing angle of  $2 \cdot 10$  mrad between the colliding beams.

## 2 Event generation

The processes under study are the pair production of scalar muons and scalar taus

$$e_L^+e_R^- \rightarrow \tilde{\mu}_R\tilde{\mu}_R \rightarrow \mu^+\tilde{\chi}_1^0\mu^-\tilde{\chi}_1^0, \quad (1)$$

$$e_L^+e_R^- \rightarrow \tilde{\tau}_1\tilde{\tau}_1 \rightarrow \tau^+\tilde{\chi}_1^0\tau^-\tilde{\chi}_1^0. \quad (2)$$

The beams are assumed to be longitudinally polarised, right-handed electrons  $e_R^-$  and left-handed positrons  $e_L^+$ , which considerably increase the production cross sections and suppress background.

The slepton decay  $\tilde{\ell}^- \rightarrow \ell^-\tilde{\chi}_1^0$  into an ordinary lepton and neutralino is isotropic and produces a flat lepton energy spectrum. The endpoint energies  $E_{+/-}$  are related to the primary slepton and the neutralino masses (neglecting the lepton mass)

$$E_{+/-} = \frac{\sqrt{s}}{4} \left( \frac{m_{\tilde{\ell}}^2 - m_{\tilde{\chi}}^2}{m_{\tilde{\ell}}^2} \right) \left( 1 \pm \sqrt{1 - 4m_{\tilde{\ell}}^2/s} \right), \quad (3)$$

$$m_{\tilde{\ell}} = \sqrt{s} \frac{\sqrt{E_- E_+}}{E_- + E_+}, \quad (4)$$

$$m_{\tilde{\chi}} = m_{\tilde{\ell}} \sqrt{1 - \frac{E_- + E_+}{\sqrt{s}/2}}. \quad (5)$$

One observes that with decreasing slepton-neutralino mass difference  $\Delta m$  the endpoint energies get lower and come closer together. For  $\tau$  decays the spectrum is quite distorted, the maximal energy of the observable particles coincides with the upper edge  $E_+$ , but the lower edge at  $E_-$  is completely diluted. However, the shape of the energy distribution can still be used to extract the  $\tilde{\tau}$  mass with high precision.

Events are generated with the program PYTHIA 6.2 [6] which includes beam polarisations  $\mathcal{P}_{e\pm}$ , initial and final state QED radiation as well as beamstrahlung à la CIRCE [7]. The decays of  $\tau$  leptons are treated by TAUOLA [8].

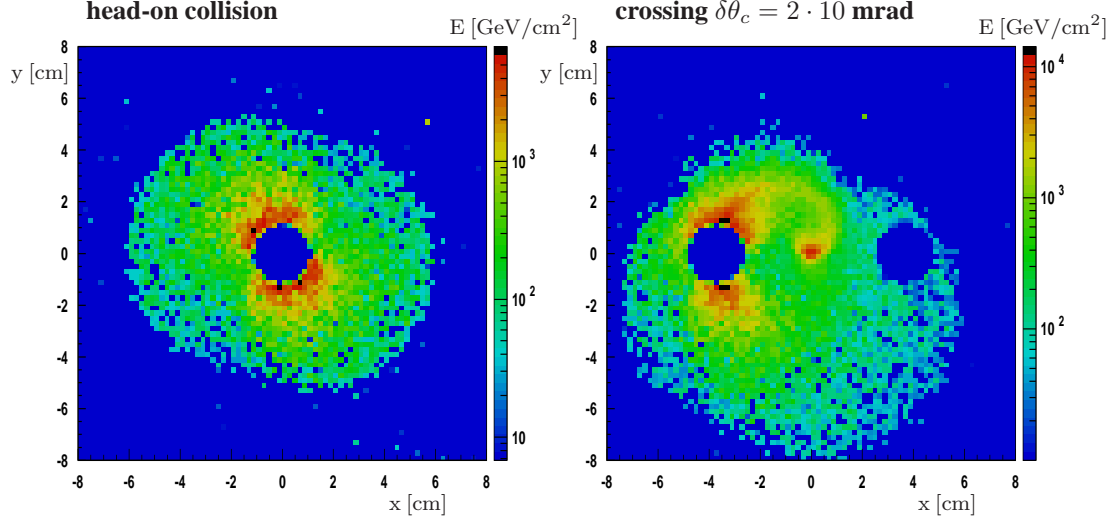


Figure 1: Energy deposits [GeV/cm<sup>2</sup>] from beamstrahlung at  $\sqrt{s} = 500$  GeV for head-on collisions (left) and crossed beams (right) in a plane perpendicular to the beams at 3.7 m from the interaction point [10]

The detector simulation is based on the detector proposed in the TESLA TDR [3] and implemented in the Monte Carlo program SIMDET 4.02 [9]. The main detector features are excellent particle identification and measurement for a polar angle acceptance  $\theta > 125$  mrad. The forward region<sup>1</sup> is equipped with electromagnetic calorimeters in order to effectively veto electrons and photons down to very small scattering angles. For  $\theta < 27.5$  mrad a highly segmented LCAL calorimeter situated at a distance of 3.7 m from the interaction point has recently been proposed [10]. For head-on collisions, as envisaged at TESLA, a beam pipe of radius  $r = 1.2$  cm appears feasible and the calorimetric coverage may start at 3.5 mrad (assuming 1 mm clearance). For beams colliding under a crossing angle of  $2 \cdot 10$  mrad there are two dead regions and the exiting, disrupted beams require a larger beampipe of  $r = 2.0$  cm, giving a minimal tagging angle of 5.7 mrad. In both cases  $e, \gamma$  tagging at low angles is very demanding above the huge background of energy deposits caused by beamstrahlung, as shown in figure 2 [10]. The beamstrahlung halo varies rapidly around the beam pipes. Further, the angle between the magnetic field and the crossed beams leads to an enhanced (factor 2) and asymmetric energy distribution. An algorithm based on topological properties of electromagnetic showers is used to veto electrons and photons a few mm close to the beam pipe for energies above 50 GeV with high efficiency [11] in both designs.

For TESLA a geometry with crossed beams is an option which may facilitate beam diagnostics. A normal conducting linear collider like NLC/GLC has to be operated with a crossing angle and the short bunch separation may lead to additional, disturbing pile up effects, depending on the calorimeter read-out. This difficulty will not be further discussed.

<sup>1</sup>The acceptance at an angle  $\theta$  in the forward region is symmetric in the backward direction at  $\pi - \theta$

### 3 Case study SPS 1a inspired model

The aim of this paper is to investigate the experimental problems related to small lepton-neutralino mass differences and to compare the results with more conventional benchmark spectra. As reference serves the mSUGRA scenario SPS 1a where detailed studies of slepton production in the continuum [12] and at threshold [13] exist. The case study is based on a SPS 1a inspired model, where the masses of the the light sleptons are kept unchanged,  $m_{\tilde{\mu}_R} = 143$  GeV and  $m_{\tilde{\tau}_1} = 133$  GeV, and the neutralino masses are increased. Within mSUGRA a  $\tilde{\tau}_1 - \tilde{\chi}_1^0$  mass splitting  $\Delta m_{\tilde{\tau}} = 8$  GeV can *e.g.* be accomplished by shifting the common gaugino mass  $m_0$  to 70 GeV and the common scalar mass  $m_{1/2}$  to 320 GeV and leaving the other parameters as  $\tan \beta = 10$ ,  $A_0 = -100$  GeV and  $\text{sign } \mu > 0$ .

The strategy will be to determine the neutralino mass from the lepton spectra of  $\tilde{\mu}_R \tilde{\mu}_R$  and/or  $\tilde{e}_R \tilde{e}_R$  production (eqs. (5) and (4)) and then use this value as input in the  $\tau$  decay spectra of the  $\tilde{\tau}$  analysis. Optimal collider operating conditions are chosen such as to maximise the signal cross section and to minimise the background: a center of mass energy of  $\sqrt{s} = 400$  GeV and beam polarisations of  $\mathcal{P}_{e^-} = +0.8$  for right-handed electrons and of  $\mathcal{P}_{e^+} = -0.6$  for left-handed positrons. Other SUSY processes are kinematically not accessible (below production thresholds) or strongly suppressed ( $\tilde{\tau}_1 \tilde{\tau}_2$ ,  $\tilde{e}_R \tilde{e}_L$  and  $\tilde{\chi}_1^0 \tilde{\chi}_2^0$ ). The SM contribution from  $WW$  production is negligible due to the beam polarisation and efficient selection criteria. The essential remaining background comes from two-photon processes  $e^+ e^- \rightarrow e^+ e^- \ell^+ \ell^-$  with cross sections of  $\mathcal{O}(10^6 \text{ fb})$ . The simulations assume an integrated luminosity of  $\mathcal{L} = 200 \text{ fb}^{-1}$ , corresponding to about one year of data taking.

#### 3.1 Detection of $e^+ e^- \rightarrow \tilde{\mu}_R \tilde{\mu}_R$

For the purpose of illustration a small smuon-neutralino mass difference of  $\Delta m = 8$  GeV is assumed. Such a situation may occur for low values of  $\tan \beta$  with the light smuon and stau being almost degenerate. The masses used in the simulation of  $e_L^+ e_R^- \rightarrow \tilde{\mu}_R^+ \tilde{\mu}_R^- \rightarrow \mu^+ \tilde{\chi}_1^0 \mu^- \tilde{\chi}_1^0$  are  $m_{\tilde{\mu}_R} = 143.0$  GeV and  $m_{\tilde{\chi}_1^0} = 135.0$  GeV. The relevant signal and background cross sections are  $\sigma_{\tilde{\mu}_R \tilde{\mu}_R} = 120 \text{ fb}$ ,  $\sigma_{WW} = 1000 \text{ fb}$  and  $\sigma_{ee\mu\mu} = 9.4 \cdot 10^5 \text{ fb}$ .

The following event selection criteria are applied: (1) veto of any electromagnetic energy ( $e$  or  $\gamma$ ) above 5 GeV in the forward region  $\theta < 125 \text{ mrad}$ , (2) two muons within the polar angle acceptance  $-0.90 < Q_\mu \cos \theta_\mu < 0.75$ , (3) acoplanarity angle  $\Delta\phi^{\mu\mu} < 160^\circ$ , (4) missing momentum vector inside active detector  $\cos \theta_{\vec{p}_{\text{miss}}} < 0.9$ , (5) muon energy  $E_\mu > 2 \text{ GeV}$ , (6) transverse momentum of di-muon system  $p_\perp^{\mu\mu} > 5 \text{ GeV}$ . The overall signal efficiency is 60 %, while the remaining background is negligible. The most effective cuts against  $WW$  production are (2) and (3). The  $\gamma\gamma \rightarrow \mu\mu$  background is reduced by a factor of  $\sim 10^{-6}$ , particularly powerful are cuts (3) and (6).

The resulting spectra of the muon energy  $E_\mu$  are shown in figure 2. The rectangular shape with the steeply rising edges is clearly observable. The background is roughly a factor of 2 larger in a configuration with beam crossing angle compared with head-on collisions. However, the influence on the endpoint energy measurements are in both cases negligible. A fit to the spectrum yields the endpoint energies  $E_- = 3.270 \pm 0.015 \text{ GeV}$  and  $E_+ = 18.480 \pm 0.39 \text{ GeV}$ ,

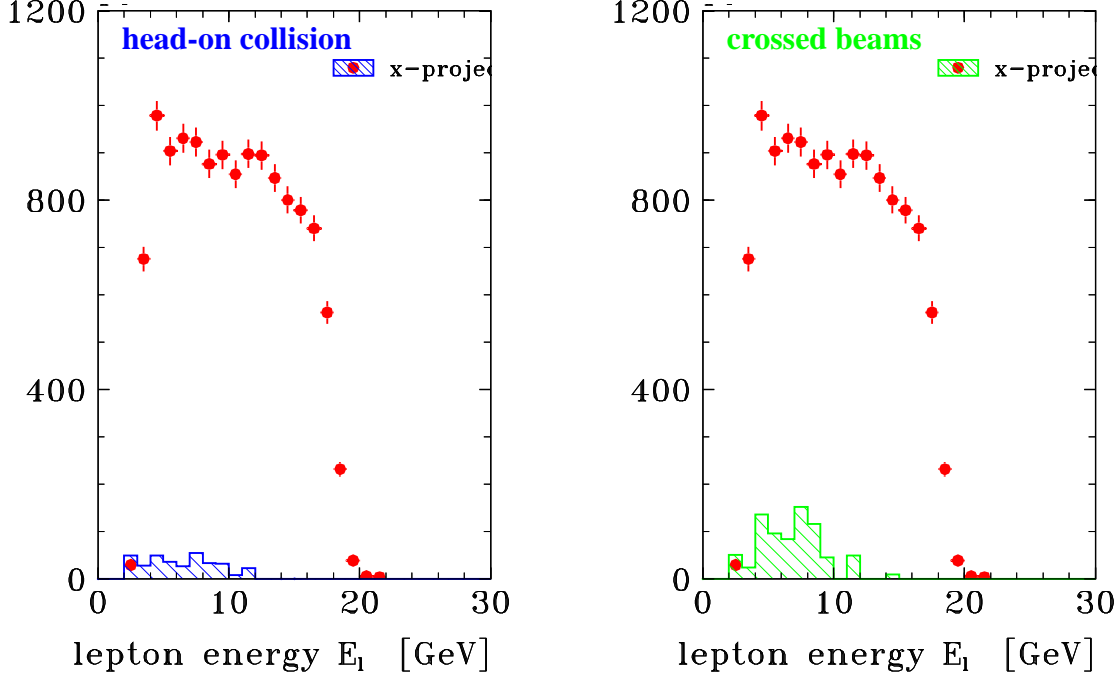


Figure 2: Muon energy spectra  $E_\mu$  from the reactions  $e_L^+ e_R^- \rightarrow \tilde{\mu}_R^+ \tilde{\mu}_R^- \rightarrow \mu^+ \tilde{\chi}_1^0 \mu^- \tilde{\chi}_1^0$  (points) and  $e_L^+ e_R^- \rightarrow e^+ e^- \mu^+ \mu^-$  (histogram) without (left) and with (right) beam crossing angle. SPS 1a inspired model,  $m_{\tilde{\mu}_R} = 143$  GeV,  $\Delta m = 8$  GeV,  $\sqrt{s} = 400$  GeV and  $\mathcal{L} = 200 \text{ fb}^{-1}$

from which the strongly correlated masses of  $\tilde{\mu}_R$  and  $\tilde{\chi}_1^0$  are derived with an accuracy of  $\delta m_{\tilde{\mu}_R} = 0.18$  GeV and  $\delta m_{\tilde{\chi}_1^0} = 0.17$  GeV, see table 1.

The precision on the neutralino mass can be considerably improved by analysing the selectron production  $e_L^+ e_R^- \rightarrow \tilde{e}_R^+ \tilde{e}_R^- \rightarrow e^+ \tilde{\chi}_1^0 e^- \tilde{\chi}_1^0$ . The cross section is roughly a factor of four higher while the two-photon background remains low. From the results of table 1 one concludes that a neutralino mass resolution of  $\delta m_{\tilde{\chi}_1^0} = 0.08$  GeV is achievable, which can be further improved by a combined analysis of both slepton production processes.

$e^+ e^- \rightarrow \tilde{\mu}_R^+ \tilde{\mu}_R^-$	$m_{\tilde{\mu}_R} = 143.0 \pm 0.18 \text{ GeV}$	$m_{\tilde{\chi}_1^0} = 135.0 \pm 0.17 \text{ GeV}$
$e^+ e^- \rightarrow \tilde{e}_R^+ \tilde{e}_R^-$	$m_{\tilde{e}_R} = 143.0 \pm 0.09 \text{ GeV}$	$m_{\tilde{\chi}_1^0} = 135.0 \pm 0.08 \text{ GeV}$

Table 1: Expected mass resolutions for  $\tilde{\mu}_R$ ,  $\tilde{e}_R$  and  $\tilde{\chi}_1^0$  from lepton energy spectra in a SPS 1a inspired scenario assuming  $\mathcal{L} = 200 \text{ fb}^{-1}$  at  $\sqrt{s} = 400$  GeV

Compared with the original SPS 1a scenario [12], the mass resolutions obtained from the first and second generation slepton pair production do not degrade with decreasing slepton-neutralino mass difference down to values of  $\Delta m = 8$  GeV, and possibly even lower to 5 GeV.

### 3.2 Detection of $e^+ e^- \rightarrow \tilde{\tau}_1 \tilde{\tau}_1$

For the simulation of  $e_L^+ e_R^- \rightarrow \tilde{\tau}_1^+ \tilde{\tau}_1^- \rightarrow \tau^+ \tilde{\chi}_1^0 \tau^- \tilde{\chi}_1^0$  a stau-neutralino mass difference of  $\Delta m = 8$  GeV is assumed, leading to  $m_{\tilde{\tau}_1} = 133.2$  GeV and  $m_{\tilde{\chi}_1^0} = 125.2$  GeV. The cross section

is  $\sigma_{\tilde{\tau}_1\tilde{\tau}_1} = 140$  fb, SM background considered have cross sections of  $\sigma_{WW} = 1000$  fb and  $\sigma_{ee\tau\tau} = 4.5 \cdot 10^5$  fb. For the identification and reconstruction of  $\tau$  pairs, one tau is required to decay into hadrons while the other may decay hadronically or leptonically. The measurement of energy spectra is restricted to the hadronic decay modes  $\tau \rightarrow \pi\nu_\tau$  (11.1%),  $\tau \rightarrow \rho\nu_\tau \rightarrow \pi^\pm\pi^0\nu_\tau$  (25.4%) and  $\tau \rightarrow 3\pi\nu_\tau \rightarrow \pi^\pm\pi^+\pi^-\nu_\tau + \pi^\pm\pi^0\pi^0\nu_\tau$  (19.4%). A difficulty may pose the  $\tau$  polarisation from  $\tilde{\tau}_1 \rightarrow \tau\tilde{\chi}_1^0$  decays, which has an influence on the pion energy spectrum, but does not affect the shape of the  $\rho$  and  $3\pi$  spectra [14]. The  $\tau$  polarisation can either be taken from calculations or can be determined simultaneously [12], if one wants to keep the pion decay channel. The leptonic 3-body decays  $\tau \rightarrow e\nu_e\nu_\tau$ ,  $\tau \rightarrow \mu\nu_\mu\nu_\tau$  exhibit a very weak dependence on  $m_{\tilde{\tau}}$  and are therefore discarded in the analysis.

The following criteria are applied to select  $\tilde{\tau}_1\tilde{\tau}_1$  events: (1) veto of any electromagnetic energy ( $e$  or  $\gamma$ ) above 5 GeV in the forward region  $\theta < 125$  mrad, (2) two  $\tau$  candidates within the polar angle  $-0.75 < \cos\theta_\tau < 0.75$ , (3) invariant mass of  $\tau$  jet  $m_\tau < 2$  GeV, (4) tau energy  $2 < E_\tau < 25$  GeV, (5) acoplanarity angle  $\Delta\phi^{\tau\tau} < 160^\circ$ , (6) missing momentum vector  $\cos\theta_{\vec{p}_{miss}} < 0.8$ , (7) transverse momentum of di-tau system  $3 < p_{\perp}^{\tau\tau} < 25$  GeV, (8) combined cut on  $\sum p_{\perp, \vec{T}}^\tau$  and  $\Delta\phi^{\tau\tau}$ . An effective reduction of  $\gamma\gamma$  background is possible by using observables defined in the plane perpendicular to the beams. Cuts (5) and (7) are not as efficient as in the smuon analysis. They have to be supplemented by criterion (8), illustrated in figure 3 as correlations between  $\sum p_{\perp, \vec{T}}^\tau$ , the sum of  $\tau$  momenta projected onto the transverse thrust axis  $\vec{T}_\perp$ , and the acoplanarity angle  $\Delta\phi^{\tau\tau}$ . A cut as indicated by the curves has little influence on the signal and reduces the background by factors of order 50. The residual  $\tilde{\tau}_1\tilde{\tau}_1$  efficiency is  $\sim 18\%$ . The two-photon background is suppressed by  $\sim 1.5 \cdot 10^{-6}$  for head-on collisions, respectively  $\sim 2.5 \cdot 10^{-6}$  in the case of crossed beams. Contributions from  $WW$  production are negligible.

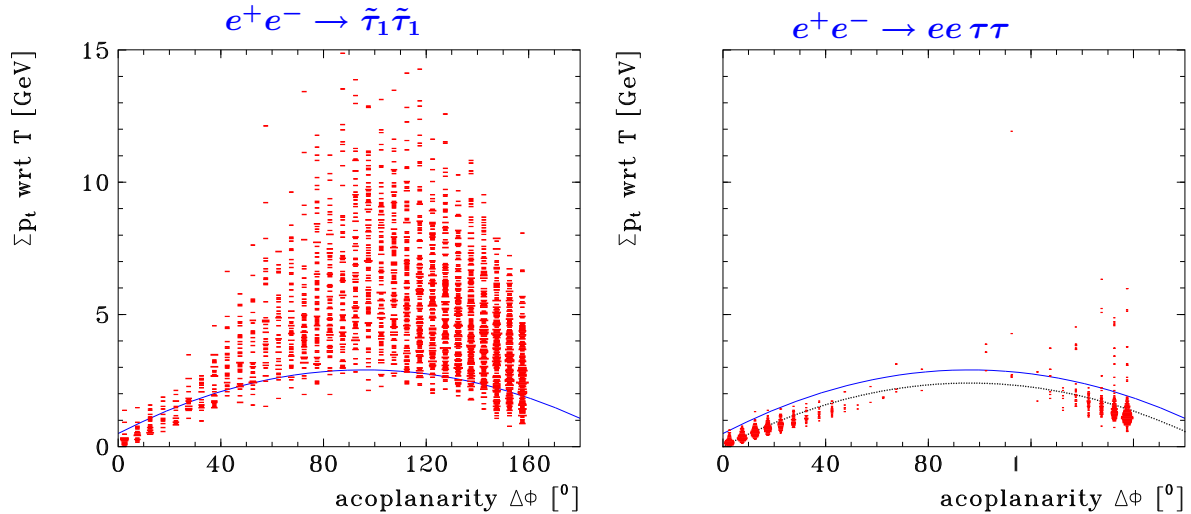


Figure 3: Correlations of  $\sum p_{\perp, \vec{T}}^\tau$  wrt thrust axis  $\vec{T}_\perp$  versus acoplanarity angle  $\Delta\phi^{\tau\tau}$  in a plane perpendicular to the beams for  $e_L^+e_R^- \rightarrow \tilde{\tau}_1\tilde{\tau}_1 \rightarrow \tau^+\tilde{\chi}_1^0\tau^-\tilde{\chi}_1^0$  (left) and  $e_L^+e_R^- \rightarrow e^+e^-\tau^+\tau^-$  (right). The curves indicate the separation between SUSY and  $\gamma\gamma$  processes. SPS 1a inspired model,  $m_{\tilde{\tau}_1} = 133$  GeV,  $\Delta m = 8$  GeV,  $\sqrt{s} = 400$  GeV

The energy spectra of  $E_\pi$ ,  $E_\rho$  and  $E_{3\pi}$  are shown in figure 4 for collisions with crossed beams. Clean signals above a very small and controllable background are observed. The spectra are fitted to full simulations with different  $\tilde{\tau}_1$  mass hypothesis, yielding a sensitivity of  $\delta m_{\tilde{\tau}_1} = 0.14 \text{ GeV} \oplus \delta m_{\tilde{\chi}_1^0}$  for the  $E_\pi$  spectrum, and  $\delta m_{\tilde{\tau}_1} = 0.10 \text{ GeV} \oplus \delta m_{\tilde{\chi}_1^0}$  for the  $E_\rho$  and  $E_{3\pi}$  spectra, each. Assuming a conservative estimate of  $\delta m_{\tilde{\chi}_1^0} = 0.10 \text{ GeV}$  one expects a combined uncertainty of  $\delta m_{\tilde{\tau}_1} = 0.14 \text{ GeV}$  for the the stau mass. A lower background expected in head-on collisions or a twofold higher rate (accounting for additional two-photon processes not covered) do not change the resolution significantly.

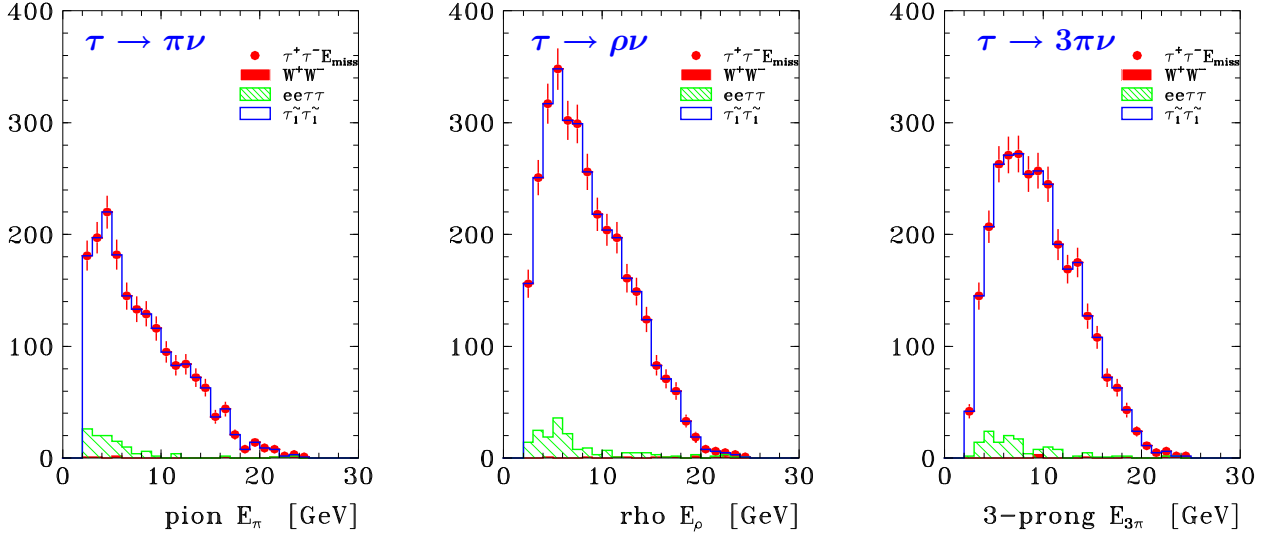


Figure 4: Hadron energy spectra  $E_\pi$  of  $\tau \rightarrow \pi \nu_\tau$ ,  $E_\rho$  of  $\tau \rightarrow \rho \nu_\tau$  and  $E_{3\pi}$  of  $\tau \rightarrow 3\pi \nu_\tau$  decays from the reactions  $e_L^+ e_R^- \rightarrow \tilde{\tau}_1 \tilde{\tau}_1 \rightarrow \tau^+ \tilde{\chi}_1^0 \tau^- \tilde{\chi}_1^0$  and  $e_L^+ e_R^- \rightarrow e^+ e^- \tau^+ \tau^-$  assuming crossed beams collision. SPS 1a inspired model,  $m_{\tilde{\tau}_1} = 133.2 \text{ GeV}$ ,  $\Delta m = 8 \text{ GeV}$ ,  $\sqrt{s} = 400 \text{ GeV}$  and  $\mathcal{L} = 200 \text{ fb}^{-1}$

It is interesting to note that the precision achieved in the present study is about twice as good as for the original SPS 1a scenario [12]. The reason is that for small stau-neutralino mass differences the energy spectra are narrower and are falling steeper at the edges. In particular, a determination of the high endpoint energy, eq. (3), is therefore more precise, which directly enters the mass calculation.

Examples of a further reduction of the stau-neutralino mass difference to  $\Delta m = 5 \text{ GeV}$  and  $\Delta m = 3 \text{ GeV}$  are shown for the  $\rho$  energy spectra in figure 5. The overall event rates decrease but are still sufficient to clearly determine the high endpoint energy. Including mass effects, the maximal  $\tau$  energy and its relation to the  $\tilde{\tau}_1$  mass are given by

$$E_+ = \frac{m_{\tilde{\tau}_1}^2 - m_{\tilde{\chi}_1^0}^2}{2(E_{\tilde{\tau}_1} - p_{\tilde{\tau}_1} f_\tau)} \quad \text{with} \quad f_\tau = 1 - 0.5(m_\tau/\Delta m)^2, \quad (6)$$

$$\delta m_{\tilde{\tau}_1} \simeq 0.38 \delta E_+ \oplus \delta m_{\tilde{\chi}_1^0}. \quad (7)$$

A very simple fit of a straight line to the upper part of the spectra yields a maximal energy of  $E_+ = 12.94 \pm 0.52 \text{ GeV}$  which translates to  $\delta m_{\tilde{\tau}_1} = 0.22 \text{ GeV}$  for a mass difference of



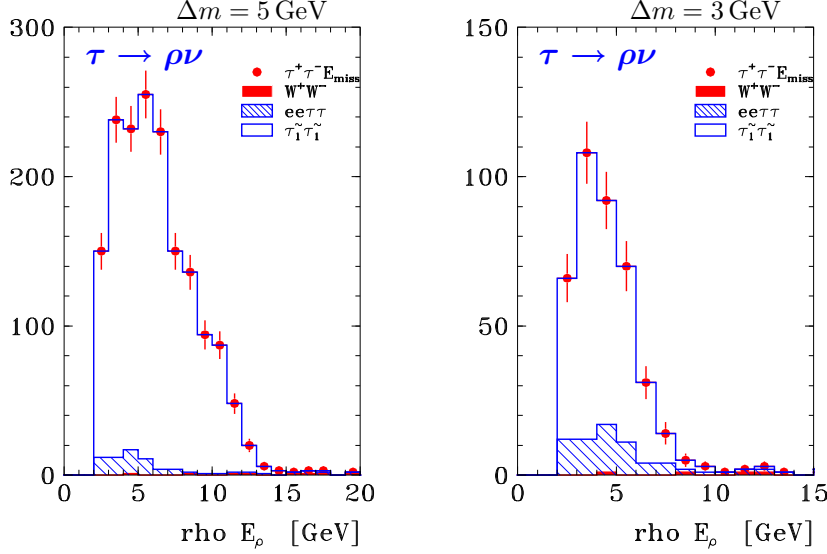


Figure 5: Hadron energy spectra  $E_\rho$  of  $\tau \rightarrow \rho \nu_\tau$  from  $e_L^+ e_R^- \rightarrow \tilde{\tau}_1^+ \tilde{\tau}_1^- \rightarrow \tau^+ \tilde{\chi}_1^0 \tau^- \tilde{\chi}_1^0$  with  $\Delta m = 5$  GeV (left) and  $\Delta m = 3$  GeV (right) assuming head-on collision. SPS 1a inspired model,  $m_{\tilde{\tau}_1} = 133.2$  GeV,  $\sqrt{s} = 400$  GeV and  $\mathcal{L} = 200 \text{ fb}^{-1}$

$\Delta m = 5$  GeV. For the scenario with  $\Delta m = 3$  GeV one obtains  $E_+ = 7.60 \pm 0.72$  GeV or  $\delta m_{\tilde{\tau}_1} = 0.28$  GeV. These resolutions for very small stau-neutralino mass differences are very encouraging and can be further improved with more refined spectra analyses. All results for the  $\tilde{\tau}_1$  mass precision obtained under different assumptions are summarised in table 2.

## 4 Case study model D'

The post-WMAP model D' [5] (parameters  $m_0 = 101$  GeV,  $m_{1/2} = 525$  GeV,  $\tan \beta = 10$ ,  $A_0 = 0$  GeV,  $\text{sign} \mu < 0$ ) is a typical benchmark in the coannihilation region. The relevant masses are the light sleptons  $m_{\tilde{\mu}_R} = m_{\tilde{e}_R} = 223.9$  GeV and  $m_{\tilde{\tau}_1} = 217.5$  GeV and the neutralino  $m_{\tilde{\chi}_1^0} = 112.4$  GeV. For the analysis the collider is chosen to operate at  $\sqrt{s} = 600$  GeV with polarised beams of  $\mathcal{P}_{e^-} = +0.8$  and  $\mathcal{P}_{e^+} = -0.6$ , which essentially suppresses all other SUSY production processes. The luminosity is assumed to be  $\mathcal{L} = 300 \text{ fb}^{-1}$ .

From the discussion of section 3.1 it is safe to conclude that the neutralino mass can be determined to an accuracy of  $\delta m_{\tilde{\chi}_1^0} \simeq 0.1$  GeV, which will be assumed in the following stau analysis.

### 4.1 Analysis of $e^+ e^- \rightarrow \tilde{\tau}_1^+ \tilde{\tau}_1^-$

The study of  $e_L^+ e_R^- \rightarrow \tilde{\tau}_1^+ \tilde{\tau}_1^- \rightarrow \tau^+ \tilde{\chi}_1^0 \tau^- \tilde{\chi}_1^0$  proceeds along the same lines as described in section 3.2. The cross section is  $\sigma_{\tilde{\tau}_1 \tilde{\tau}_1} = 50 \text{ fb}$ . The event selection is identical except a tighter cut (6) on the tau energy of  $2 < E_\tau < 15$  GeV, due to the small stau-neutralino mass difference



$\Delta m = 5.1$  GeV. The resulting overall efficiency is 7.6 %. In addition to  $e^+e^- \rightarrow e^+e^-\tau\tau$  a hadronic background from two-photon quark production  $\gamma\gamma \rightarrow q\bar{q}$  is included. The major contribution comes from charm quarks where the final states mimic a tau pair. There is still an uncertainty on some missing graphs concerning real or ‘direct’  $\gamma\gamma$  interactions, which may contribute with a similar magnitude. Fortunately, the total background can be kept small at a few percent level, and an increase by a factor of  $\sim 1.5$  would not change the results significantly. In a final experiment the  $\gamma\gamma$  background will be precisely measurable and should be reliably calculable.

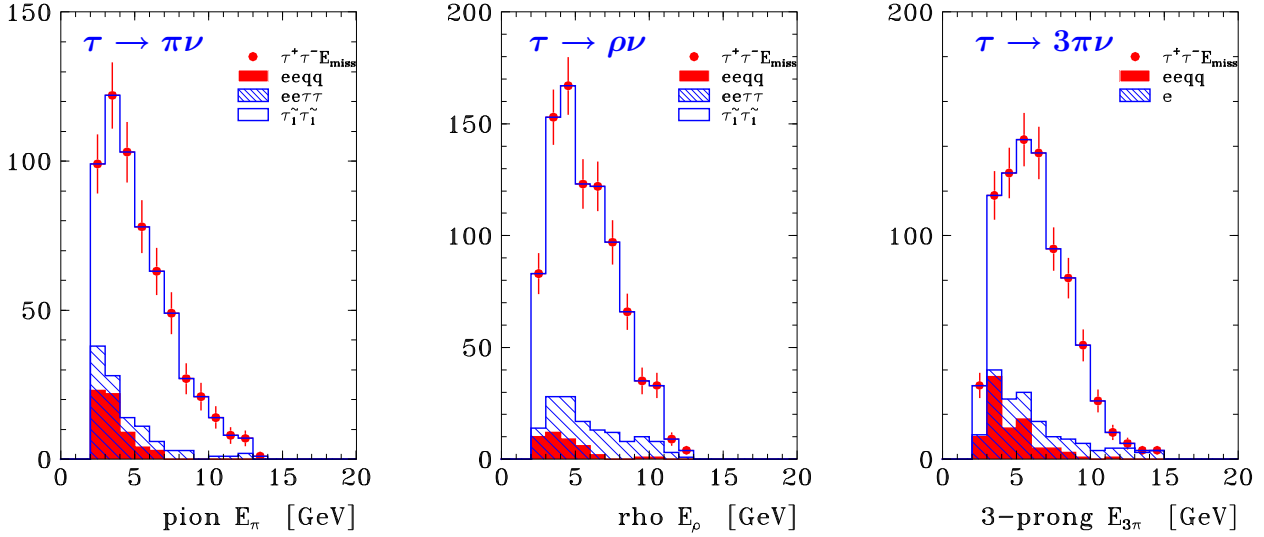


Figure 6: Hadron energy spectra  $E_\pi$  of  $\tau \rightarrow \pi\nu_\tau$ ,  $E_\rho$  of  $\tau \rightarrow \rho\nu_\tau$  and  $E_{3\pi}$  of  $\tau \rightarrow 3\pi\nu_\tau$  decays from the reaction  $e_L^+e_R^- \rightarrow \tilde{\tau}_1\tilde{\tau}_1 \rightarrow \tau^+\tilde{\chi}_1^0\tau^-\tilde{\chi}_1^0$  and two-photon production assuming head-on collision. Model D',  $m_{\tilde{\tau}_1} = 217.5$  GeV,  $\Delta m = 5.1$  GeV,  $\sqrt{s} = 600$  GeV and  $\mathcal{L} = 300 \text{ fb}^{-1}$

The energy spectra of  $E_\pi$ ,  $E_\rho$  and  $E_{3\pi}$  are shown in figure 6 for head-on collisions. One observes narrow distributions with a small background increasing towards low energies. From fits to the spectra assuming various  $\tilde{\tau}_1$  mass hypothesis, one obtains uncertainties in the mass determination of  $\delta m_{\tilde{\tau}_1} = 0.19 \text{ GeV} \oplus \delta m_{\tilde{\chi}_1^0}$  for the  $E_\pi$  spectrum,  $\delta m_{\tilde{\tau}_1} = 0.12 \text{ GeV} \oplus \delta m_{\tilde{\chi}_1^0}$  for the  $E_\rho$  spectrum and  $\delta m_{\tilde{\tau}_1} = 0.14 \text{ GeV} \oplus \delta m_{\tilde{\chi}_1^0}$  for the  $E_{3\pi}$  spectrum. Combining the information of all measurements and folding in the neutralino mass error ( $\delta m_{\tilde{\chi}_1^0} = 0.1 \text{ GeV}$ ) the stau mass can be determined as  $m_{\tilde{\tau}_1} = 217.5 \pm 0.15 \text{ GeV}$ . Despite the lower event rates the achievable accuracy is very similar to that obtained for the SPS 1a inspired model (see section 3.2). This supports the observation that narrow distributions have a somewhat higher analysing power. The results of the simulation of model D' are given in table 2.

## 5 Conclusions

Simulations of slepton production  $e^+e^- \rightarrow \tilde{\mu}_R\tilde{\mu}_R$  and  $e^+e^- \rightarrow \tilde{\tau}_1\tilde{\tau}_1$  in scenarios with small slepton-neutralino mass differences  $\Delta m$  are presented under realistic experimental conditions.

scenario	$m_{\tilde{\tau}_1}$ [GeV]	$\delta m_{\tilde{\tau}_1}$ [GeV]	$\Delta m$ [GeV]	$\delta \Omega_{CDM} h^2$
SPS 1a inspired	133.2	0.14	8	1.7 %
		0.22	5	4.1 %
		0.28	3	6.7 %
model D'	217.5	0.15	5.1	1.9 %

Table 2: Expected accuracies on the stau mass  $\delta m_{\tilde{\tau}_1}$  and the resulting precision on dark matter density  $\delta \Omega_{CDM} h^2$  for variants of a SPS 1a inspired scenario ( $\mathcal{L} = 200 \text{ fb}^{-1}$  @ 400 GeV) and the benchmark model D' ( $\mathcal{L} = 300 \text{ fb}^{-1}$  @ 600 GeV)

Choosing the proper collider energy and beam polarisations, the decay lepton energy spectra are analysed and allow the masses of the light sleptons and the neutralino  $\tilde{\chi}_1^0$  to be determined very precisely, to an accuracy of one per mil. The results of various case studies with ranges  $\Delta m = 8 \text{ GeV} \rightarrow 3 \text{ GeV}$  are summarised in table 1 and table 2.

Methods are devised to efficiently suppress the most serious background from  $\gamma\gamma$  four-fermion production  $e^+e^- \rightarrow e^+e^-f\bar{f}$ , with  $f = \mu, \tau, q$ , which becomes more important with decreasing  $\Delta m$ . It is mandatory to have excellent veto capabilities for the scattered  $e^\pm$  down to very small angles as close as possible to the beam pipe. Low angle tagging can be more easily achieved in head-on collisions of the TESLA design. In the case of a crossing angle of  $2 \cdot 10 \text{ mrad}$  the  $\gamma\gamma$  background is larger by a factor of  $1.5 - 2$ . However, one does not expect significant degradations of the mass resolutions as long as the background can be kept small, say  $\lesssim \mathcal{O}(10\%)$ .

For the model D', which is typical for the coannihilation region, the achievable  $\tilde{\tau}$  mass resolution from energy spectra is  $\delta m_{\tilde{\tau}_1} = 0.15 \text{ GeV}$ . The present analysis can be compared with an alternative method, based on a cross section measurement of  $\tilde{\tau}_1\tilde{\tau}_1$  production close to threshold [15]. Under favourable conditions and assuming a luminosity of  $500 \text{ fb}^{-1}$  an accuracy of  $0.54 \text{ GeV}$  is quoted, which is considerably worse than the value obtained from energy spectra of the decay particles.

It is interesting to put the results in the context of a dark matter scenario. Within the coannihilation region the dark matter content of the universe is essentially determined by  $\Delta m$ , respectively the masses  $m_{\tilde{\tau}_1}$  of the stau and  $m_{\tilde{\chi}_1^0}$  of the neutralino. A calculation of the relic dark matter density with the program MICROMEGAS [16] and using the uncertainties of the present study shows that  $\Omega_{CDM} h^2$  can be predicted at the few percent level, see table 2. This emphasises the important role of a future TeV Linear Collider to provide high precision measurements.

**Acknowledgement** I want to thank Z. Zhang for valuable discussions concerning some aspects on tau detection and two-photon physics, K. Büßer for supplying the calculations of background caused by beamstrahlung, and V. Drugakov for providing the efficiency functions of the calorimeter surrounding the beam pipe.

## References

- [1] D. N. Spergel *et al.* [WMAP collaboration], *Astrophys. J. Suppl.* **148** (2003) 175.
- [2] H. Baer, A. Belyaev, T. Krupovnickas and X. Tata, *JHEP* **0402** (2004) 007; H. Baer, A. Belyaev, T. Krupovnickas and J. O’Farrill, hep-ph/0405210.
- [3] TESLA Technical Design Report, DESY 2001-011, Part III: *Physics at an  $e^+e^-$  Linear Collider* [hep-ph/0106315], Part IV: *A Detector for TESLA*.
- [4] B.C. Allanach *et al.*, *Eur. Phys. J. C* **25** (2002) 113;  
N. Ghodbane, H.-U. Martyn, hep-ph/0201233.
- [5] M. Battaglia *et al.*, *Eur. Phys. J. C* **33** (2004) 273.
- [6] T. Sjöstrand *et al.*, *Comput. Phys. Commun.* **135** (2001) 238.
- [7] T. Ohl, *Comput. Phys. Commun.* **101** (1997) 269.
- [8] S. Jadach *et al.*, *Comput. Phys. Commun.* **76** (1993) 361.
- [9] M. Pohl, J. Schreiber, DESY-02-061, hep-ex/0206009.
- [10] K. Büßer, talk at the *International Conference on Linear Colliders*, LCWS 04, Paris, April 2004.
- [11] V. Drugakow, private communication.
- [12] H.-U. Martyn, hep-ph/0406123 [LC-PHSM-2003-071].
- [13] A. Freitas, A. von Manteuffel and P. M. Zerwas, *Eur. Phys. J. C* **34** (2004) 487.
- [14] M.M. Nojiri, *Phys. Rev. D* **51** (1995) 6281;  
M.M. Nojiri, K. Fujii, T. Tsukamoto, *Phys. Rev. D* **54** (1996) 6756.
- [15] P. Bambade, M. Berggren, F. Richard and Z. Zhang, hep-ph/0406010.
- [16] G. Bélanger *et al.*, hep-ph/0405253 and *Comput. Phys. Commun.* **149** (2002) 103.